EARTHQUAKE ENGINEERING AND STRUCTURAL DYNAMICS
Earthquake Engng. Struct. Dyn. **28**, 1685–1704 (1999)

VERTICAL OSCILLATIONS DUE TO AXIAL-BENDING COUPLING DURING SEISMIC RESPONSE OF RC BRIDGE PIERS

GIULIO RANZO*†, MARCO PETRANGELI‡ AND PAOLO EMILIO PINTO§
Department of Structural and Geotechnical Engineering, University of Rome 'La Sapienza', Via Gramsci 53, 00197 Rome, Italy

SUMMARY

The paper presents a numerical investigation on the behaviour of reinforced concrete bridge piers subjected to horizontal seismic input. Scope of the investigations is to quantify the phenomenon of bending-induced axial vibrations. The results of a set of analyses conducted on single-column bent systems indicate that flexural cracking produces, in fact, significant axial vibrations. This effect is particularly relevant in squat elements with low axial force where the sway of the cross-sectional neutral axis under alternate bending causes strong hammering impulses at crack closure. Quantification of the effects related to this phenomenon can be determinant for the seismic assessment of existing bridges as well as for the design of new bridges. Likewise, performance and design forces of bearings and other anti-seismic devices can be estimated with more accuracy, based on the expected level of combined vertical and horizontal acceleration response on decks. The pier overall flexural response is not significantly altered by the fluctuation in axial force associated to these impulses, although local moment–curvature behaviour is, due to axial–bending interaction. Shear resisting mechanisms should be more sensitive to these vibrations and shear failure anticipated when a reduction in the axial contribution to the section shear capacity occurs. A tentative equation for the prediction of this flexural-induced vertical acceleration component is proposed based on simplified section kinematics and elastic impact analysis.

KEY WORDS: axial vibrations; vertical accelerations; vertical ground motion

INTRODUCTION

In view of the field evidence[1] of the damaging effects due to axial vibrations in vertical members of RC structures during past earthquakes, various authors have investigated this problem in the past few years. In particular, the effects of vertical ground motion components on buildings and bridges[2,3] have been studied. The ground motion vertical component tends, in general, to be

* Correspondence to: Giulio Ranzo, Department of Structural and Geotechnical Engineering, University of Rome 'La Sapienza', Via San Godenzo 65, Rome I-00189, Italy
† PhD Student, University of Rome 'La Sapienza', Rome, Italy
‡ Assistant Professor, University of Chieti 'G.D'Annunzio', Pescara, Italy
§ Professor of Earthquake Engineering, University of Rome 'La Sapienza', Rome, Italy

Received 13 August 1998
CCC 0098–8847/99/121685–20$17·50 *Revised 16 March 1999*
 Accepted 24 March 1999

ignored or underestimated in current seismic analysis of structures. On the contrary, some studies have shown that it has a considerable relevance, particularly in the field of soil–structure interaction.[4] A remarkable field evidence of this fact was found in the near past, during the Hyogo-ken Nanbu earthquake of 1995, where[5] ground vertical acceleration components experienced little attenuation from bedrock to ground surface (as opposed to horizontal ones), even in potentially liquefiable soils. As a consequence, high vertical seismic inputs on structures were observed and unusual failures of vertical members occurred.

While a number of studies has been presented on the effects of vertical ground motion on structures in general,[6] little or no attention has been dedicated to vertical accelerations induced in RC members by flexural cracking. Independently of the vertical ground motion input, this source of vertical impulses can cause particularly severe effects in some types of structures. For a realistic estimate of the global response of RC structures, the two components outlined above should be added together.

Most seismic codes do not give, in fact, specific recommendations on this issue. Nonetheless, structural members may experience sudden failures associated with instantaneous decay of shear or flexural strength due to high axial force fluctuations. As reported in Reference 7, axial force fluctuations due to the effect of vertical ground motion may easily exceed $\pm$ 60 per cent of the static axial load. In these circumstances, the piers become obviously very vulnerable. Moreover, maximum bending-induced vertical accelerations should occur approximately at maximum horizontal response, therefore determining a case of extreme severity. The issue is particularly relevant when considering the performance of joints and bearings.

Scope of the present work is to quantify the component of vertical oscillations due to concrete cracking and rocking mechanism in bridge piers, with particular reference to systems in which the deck is made of multiple girders supported by large cap beams. In this kind of structures, very frequent in European and Japanese highway networks, bending-induced axial vibrations may have a significant effect on the general structural performance. The frequency content and magnitude of the vertical motion associated with this effect is analysed for different structures, with different natural periods. Consequences on the performance of bearings is also investigated. Typical existing viaducts, as well as similar structures, designed using Eurocode 8 seismic code provisions[9] are analysed. A simplified model, based on the cracked section kinematics, is developed to predict the magnitude of bending-induced axial accelerations.

THE ANALYSED STRUCTURES: GEOMETRY AND DIMENSIONING

Three different structures, meant to be representative of typical prestressed concrete viaducts in seismic regions, have been analysed. The three structures have the same 30 m span superstructure and different pier heights: 6, 12 and 18 m, respectively. Each analysed structure is supposed to be part of a viaduct made of a sequence of equal spans, simply supported on piers of similar heights. The analysis of the seismic response of these structures in the transverse direction is then carried out on a 2D schematization, taking into consideration one pier only with two half spans each side.

The superstructure, with a total platform width of 15·7 m, is made of a 0·25 m reinforced concrete slab connecting four prestressed concrete girders as shown in Figure 1. This deck configuration requires a 11·5 m wide cap beam, in order to seat four bearings with a centre to

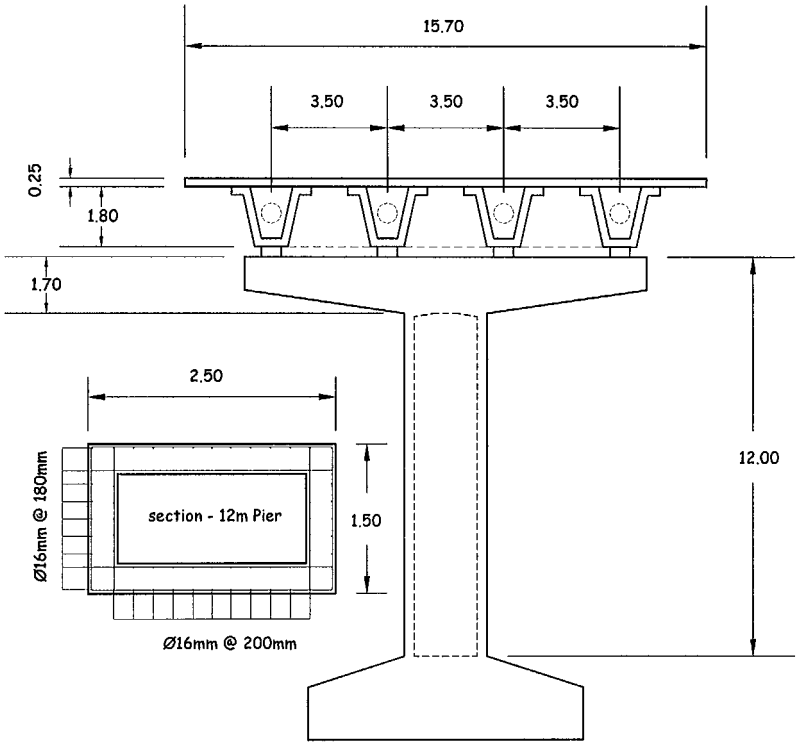

Figure 1

centre distance of 3·5 m. The weight of one span has been assumed equal to 6000 kN, therefore a vertical load of 1500 kN acts on each bearing support. An additional weight of 600 kN has been considered to account for the cap beam.

Dimensioning of the pier cross section has been carried out so as to obtain a normalized axial load $P/f_c' A_g = 0{\cdot}1$ under self-weight alone, as typical for this kind of structures (f_c' is the unconfined concrete compression strength and A_g is the area of the gross section). The flexural capacity of the pier cross section, reflecting the actual situation of most existing viaducts, has been dimensioned according to allowable stress criteria. For each structure, the design moment is computed based on a constant response spectrum of 0·1 g. The required flexural capacities are therefore proportional to the pier height since the total mass is roughly the same for the three cases; the base bending moments are computed on a cantilever scheme, neglecting the influence of deck torsional inertia and cap beam flexibility.

The same hollow cross section has been adopted in the three cases with different amount of longitudinal reinforcing steel ρ_l. Table I summarizes the main design characteristics.

Note that the longitudinal reinforcement ratios have been expressed as a function of the concrete section net area (excluding the hollow portion). The first yield moment M_y (bending moment at first yield of longitudinal rebars) and the nominal moment M_n (defined here as the bending moment at 5 times yield curvature) are indicated to conventionally define the mechanical properties.

Table I. Pier geometry and mechanical properties

Pier height (m)	Section dimensions (m)	Wall thick. (m)	ρ_l (%)	M_y (kNm)	M_n (kNm)
6	2·5 × 1·5	0·3	0·35	9667	10 166
12	2·5 × 1·5	0·3	0·70	12 204	13 939
18	2·5 × 1·5	0·3	1·00	14 090	16 929

Table II. EC8 dimensioning

Pier height (m)	M_d (kNm) — EC8	Behav. factor q
6	13 300	2·5
12	10 941	3·5
18	10 002	3·5

The choice of this kind of structures, with extremely low longitudinal reinforcement, reflects the intention of approaching the problem from the assessment of existing bridge piers. The use of current design codes based on ultimate limit state analysis and period-dependent response spectra would lead, in fact, to different flexural capacities. For comparison, the design moments obtained using the EC8 Design Code[9] for a peak ground acceleration of 0·35 g, are reported in Table II.

Following the EC8 design procedure, design moments M_d have been computed using modal analysis of the structure including cap beam flexibility and lumped masses with horizontal as well as vertical components. A reduced ductility level (behaviour factor q) has been used for the 6 m pier as suggested by the EC8 in case of squat members.

Shear dimensioning of the three structures is omitted since the investigations are focused on axial–flexural coupling, however, it is assumed that adequate shear reinforcement is provided to ensure a flexural dominant response when large inelastic displacements occur.

Before analysing the non-linear behaviour of these structures under a selected earthquake, it is interesting to see the results of the modal analysis to gain an insight on their dynamic properties. When these structures are modelled with realistic flexibility for the cap beam and both vertical and rotational masses are included to account for the vertical loads of the superstructure acting on the bearing supports, higher modes significantly influence the global behaviour. Especially in the case of the short pier, a significant percentage of horizontal modal mass is found in the second mode, which is of the double bending type. In the following, the important consequences of these aspects on the phenomenon of bending-induced axial vibrations will be discussed.

Two different configurations have been analysed for the structural systems under consideration: the first assumes an infinitely rigid superstructure (rigid deck model), the second assumes a realistic flexibility for the superstructure (flexible deck model). The corresponding mass and stiffness distributions are represented in Figures 2 and 3, respectively. The main difference between the two models is that vertical masses are rigidly connected to the pier cap beam in one case, and via elastic supports (simulating the deck flexibility in the vertical plane) in the other case.

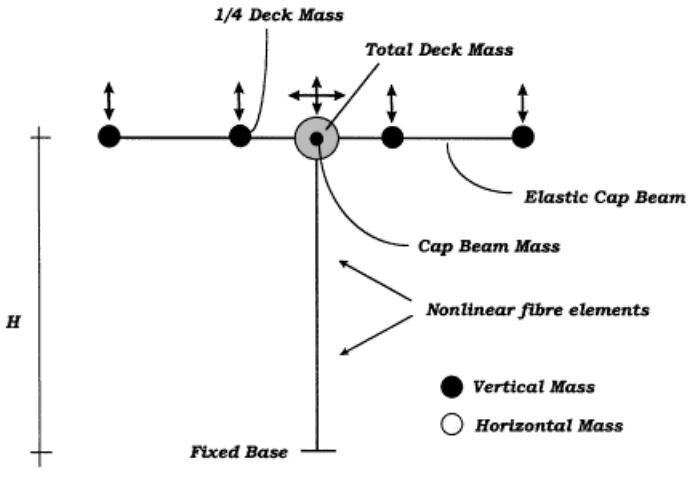

Figure 2. Rigid deck model

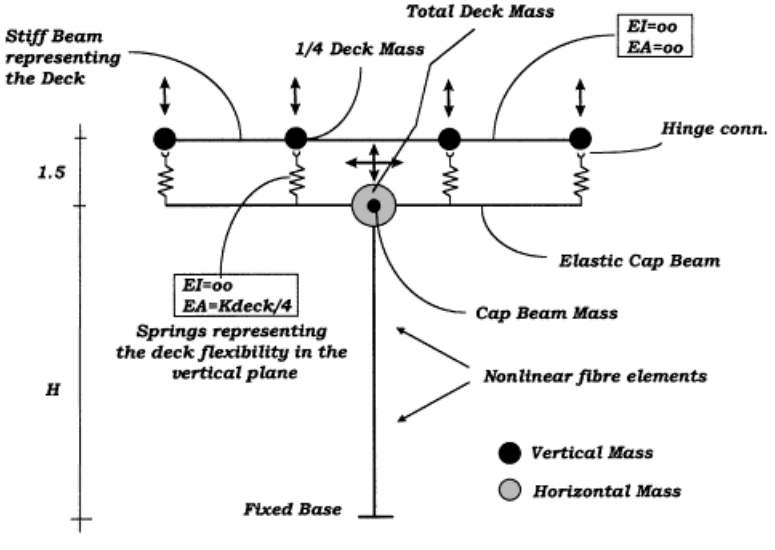

Figure 3. Flexible deck model

Natural frequencies and participating masses in the x and y direction are indicated in Table III for the two models. The mode shapes of the 6 m pier structure are depicted in Figure 4 both in the case of rigid and flexible deck assumption.

As anticipated before, it can be noted that the horizontal mass has a relatively low contribution to the first mode in the 6 m pier (especially in the flexible deck assumption). Rotation of the pier top is very limited in this case, thus enforcing a reverse bending behaviour. Concrete cracking will therefore take place in the top and bottom sections, possibly increasing the hammering effect at

Table III. Results of modal analyses

Pier height (m)	Mode number	Participating mass % — X dir.	Participating mass % — Y dir.	T (sec)
		Rigid deck		
6	1	51·0	—	0·583
6	2	48·0	—	0·123
6	3	—	76·0	0·070
12	1	79·9	—	1·190
12	2	20·1	—	0·232
12	3	—	90	0·090
18	1	89·9	—	1·960
18	2	10·1	—	0·303
18	3	—	95	0·104
		Flexible deck		
6	1	36·0	—	0·637
6	2	—	87·0	0·322
6	3	59·0	—	0·243
12	1	76·2	—	1·220
12	2	23·1	—	0·363
12	3	—	84·0	0·326
18	1	88·7	—	1·970
18	2	11·1	—	0·427
18	3	—	82·0	0·330

bending reversal. In the 12 and 18 m piers instead, the deck rotational inertia is not significant when compared to the pier flexibility. The pier deforms mainly in simple bending with concrete cracking located at pier base only.

In all linear elastic modal analyses, cracked stiffnesses have been assumed for the pier section using the expressions proposed in Reference 10.

Particular attention has been given to the modelling and to the distribution of lumped masses, since axial vibrations on the pier might excite vertical vibration modes. For this reason it has been decided to also investigate the influence of deck flexibility.

THE NUMERICAL MODELS FOR NON-LINEAR TIME-HISTORY ANALYSES

The three structures have been modelled using a flexibility-based fibre beam element developed by the authors.[11,12] The peculiarity of this element being that equilibrium, compatibility and constitutive equations are satisfied along the element, at each load increment, using an equilibrium-based iterative solution.[13] This feature is particularly relevant to the problem under

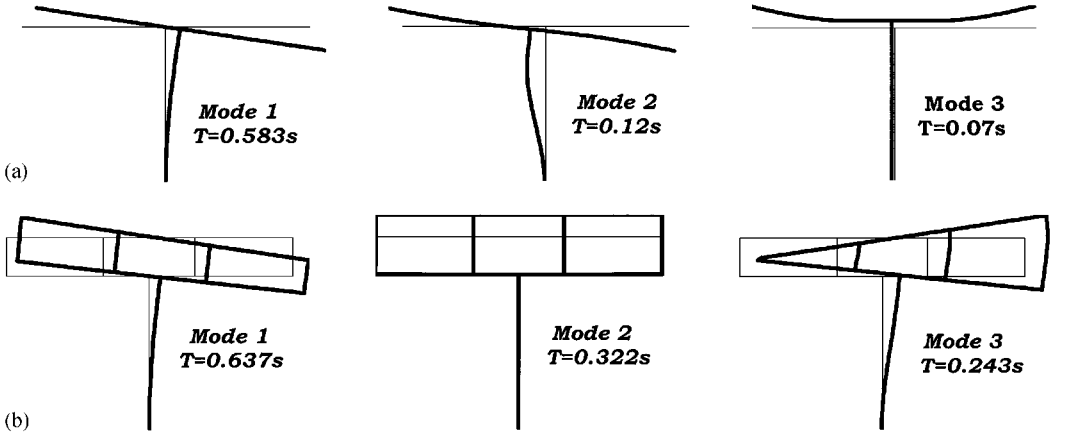

Figure 4. (a) Rigid deck model — modal shapes; (b) Flexible deck model — modal shapes

consideration since, using the traditional stiffness approach, the axial force impulse associated with the non-linear flexural behaviour would result in an internal element unbalance which would not be correctly integrated along the element length.

Each pier has been modelled using two fibre beam elements with three, four and five integration Gauss points (monitoring sections) for the 6, 12 and 18 m piers, respectively. The number of integration points has been selected in order to attain the same numerical precision in integrating the longitudinal strain field in the three structures, while maintaining the same tributary length to each integration point. The integration of the element strain field would require in fact a larger number of integration points for the shorter piers which have a predominant double bending type of deformation compared to the single bending type of the taller ones. The opposite would be required to keep a constant tributary length for each monitoring section. In fact, in the shorth pier shear cracking will take place over at least 2/3 of column height, indicating the presence of a larger plastc hinge region. On the other side, the extremely low longitudinal reinforcement ratio will localize plastic hinging at the base. As a consequence, it is believed that, in this specific case, the suggested integration scheme applies successfully to all three piers.

The pier cap has been modelled using linear elastic elements with equivalent mechanical properties. Rigid offsets have been introduced to account for the pier cross section width and the pier cap height. Constitutive models for concrete and reinforcing steel use state-of-the-art uniaxial stress–strain relationships based on the work of Mander[14] and Menegotto-Pinto,[15] respectively (see also Figures 6 and 7). In the concrete model, a crack-bridging branch has been introduced, providing a smooth transition between the tensile and the compression branches. This feature was required in order to avoid an overestimation of the impulsive component of vertical acceleration at crack closure which the original concrete model could have caused as a result of the abrupt transition between the zero stiffness, zero stress-cracked state and the reloading branches to compression.

Mechanical properties of the steel have been assumed as follows: yield strength = 400 MPa, ultimate strength = 570 MPa, Young's modulus = 200 000 MPa, ultimate strain = 0·10. Mechanical

properties of the concrete are: unconfined strength = 35 MPa, confined strength = 42 MPa, strain at ultimate stress = 0·0035, Young's modulus = 30 000 MPa, tensile strength = 2·5 MPa, fracture energy = 0·1 kN/m.

The deck horizontal mass (600 t) has been placed in one node only (at pier top, as indicated in Figures 3 and 4) to avoid axial (horizontal) vibrations in the pier cap beam; vertical masses have been placed instead at each beam support (150 t each) and at pier top (60 t). In the rigid deck model, the mass of the superstructure is rigidly connected to the cap beam (Figure 2). In the flexible deck model instead, deck vertical masses are connected to the cap beam via elastic supports (Figure 3). The stiffness of these elastic supports has been assumed such that the vertical oscillation of the rigid horizontal beam representing the superstructure (upper beam in Figure 3), has the same period of the first vertical mode of a typical prestressed concrete deck of 30 m span; this period is estimated at 0·3 sec.

The first-mode natural frequencies computed with modal analysis have been used to quantify the viscous component of the structural damping. A viscous damping, in addition to the hysteretic one, has been considered in fact by means of a mass proportional damping factor C, where, for elastic systems, $C = 2\xi\omega m$ with m the mass, ξ the percentage of critical damping and ω the circular frequency. A value of 3 per cent of critical damping has been assumed in our case to be representative of all viscous damping components acting within the elastic structural response. This value adds up to the significant energy dissipation provided by the hysteretic behaviour of concrete in tension (fracture and bond energy). It mainly accounts for the damping effects caused by deformation in the bearings, in the cap beam and in the deck.

RESULTS OF NON-LINEAR ANALYSES

A set of non-linear time-history analyses using the general purpose F.E. code FIBER (developed at University of Rome[11]) has been performed using an accelerogram compatible with the EC8 response spectrum with PGA = 0·35 g as horizontal ground motion input. The vertical component has been purposely ignored in a first stage, while it has been included in a second set of analyses to evaluate the coupling effect on the pier axial response. A generated accelerogram, rather than a natural one, has been considered for the reason of simplicity. Several different ground motion inputs should be considered in fact for a more complete analysis.

Under the imposed horizontal ground motion, large inelastic deformations occur in the three structures. In all cases a plastic hinge forms at pier base, where longitudinal reinforcing bars reach (for the 6 m pier) a maximum strain of approximately 2·0 per cent. Maximum base shears are 2500, 1250 and 980 kN for the 6, 12 and 18 m pier, respectively.

Moment curvature cycles at pier base are plotted in Figure 5 for the rigid deck models. In the same graphs the corresponding axial force time history is also reported. The largest ductilities are found for the 6 m pier with a curvature ductility $\mu_\phi = 8$–9. For this pier, the inflection point is located at 0·54 H (with H full height of the pier), while for the 12 and 18 m it is 0·66 and 0·69 H, respectively. Note that the maximum axial force fluctuations are found for the 6 m pier ($+58$ per cent in compression and -35 per cent in tension). None of the piers experienced steel yielding in the top section below the pier cap beam. Concrete and steel stress–strain histories for the base section of the 6 m pier are plotted in Figures 6 and 7.

In the 6 m pier a global displacement ductility of about 5·0 is reached, compared to 2·5 and 2·0 in the 12 and 18 m pier, respectively. This remarkable difference in global damage is due to the

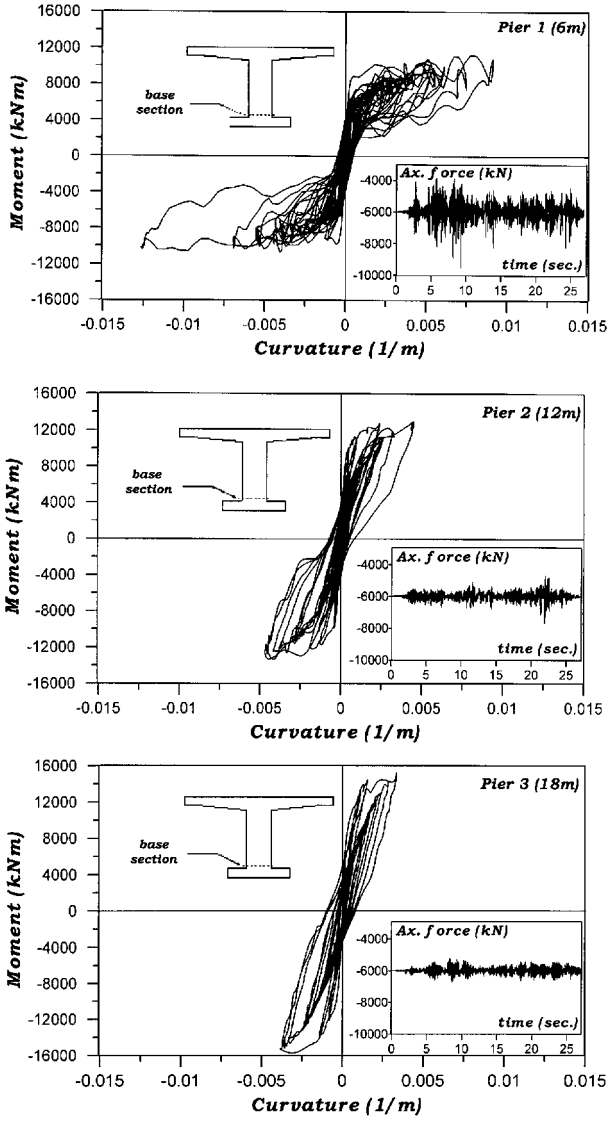

Figure 5

inappropriate strength provided by the allowable stress design criterion and to the flat design spectrum adopted (0·1 g). However, this result reflects the actual situation on existing viaducts where squat piers tend to have very light longitudinal reinforcement ratios.

Maximum displacements drifts are in a range of 0·75–1 per cent of pier height. Maximum vertical displacements at external bearing locations are insensitive to the pier height and are always around 0·05 m.

The maximum response of the three structures is summarized in Figures 9 and 10 for the rigid deck and flexible deck model, respectively. Maximum accelerations at bearing locations are

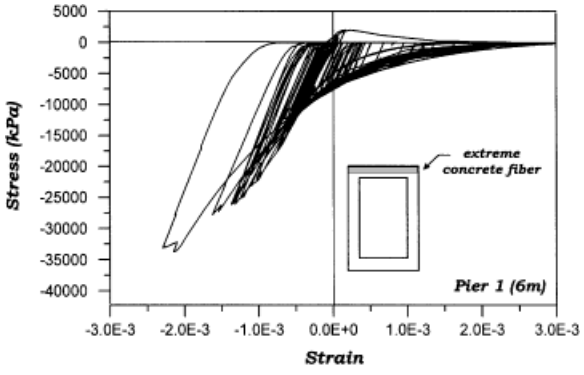

Figure 6

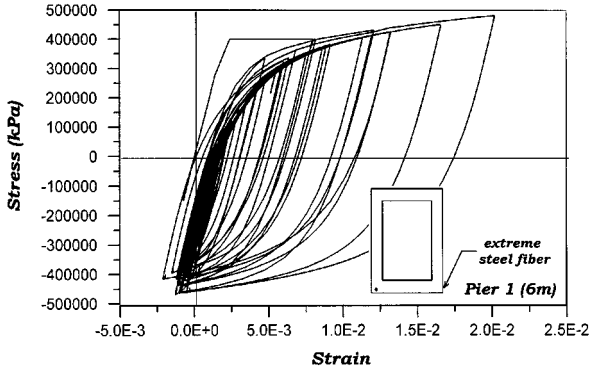

Figure 7

indicated for each structure as a function of their fundamental elastic flexural period. It can be seen that in the proposed examples, the deck horizontal maximum acceleration does not vary significantly with pier height while the vertical acceleration does, due to varying axial/flexural period ratio as well as cap beam width/pier height ratio.

As anticipated before, vertical acceleration response is particularly high for the squat pier, where a peak value of 0·9 g is found at external bearing location. Generally, bending-induced vertical accelerations decrease with increasing pier height as also confirmed by other analyses. Vertical acceleration of the outer bearings includes in fact both an amplification of the pier vertical acceleration due to the pier cap beam flexibility and a 'geometric' component due to the rotational acceleration of the pier cap beam itself. This component obviously decreases with decreasing cap beam width/pier height ratio. The distribution of the vertical acceleration along the cap beam from pier top to external bearing location can easily be derived from the graphs of Figure 8. In Figures 8 and 9 the elastic response spectrum (with 5 per cent damping) corresponding to the generated accelerogram used in the analyses as ground motion input, is also reported.

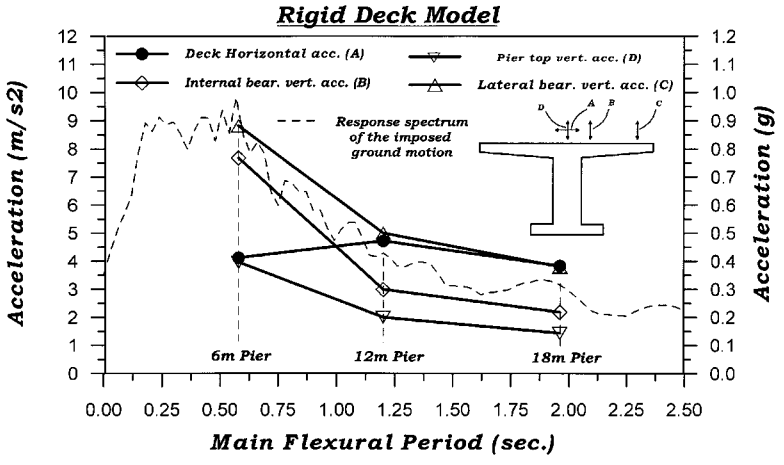

Figure 8

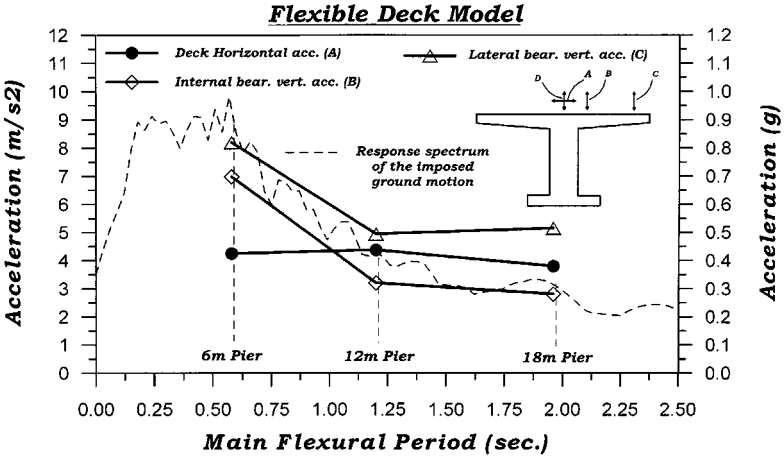

Figure 9

Minor differences between the rigid and flexible deck models in terms of maximum accelerations are detected, although for the 18 m pier, the vertical acceleration on the outer bearing is higher due to dynamic amplification.

Maximum vertical response at pier top for the flexible deck model (see Figure 9) has been omitted since no significant mass is lumped in that location. Results seem to indicate that, in this kind of structures, the deck flexibility does not influence the structural response in the vertical plane. However, it has to be noted that other imposed ground motions might induce a different response, leading to different conclusions.

Maximum displacement envelopes are shown in Figure 10 for rigid and flexible deck models. It should be noted that both the maximum horizontal and vertical displacements mainly depend on

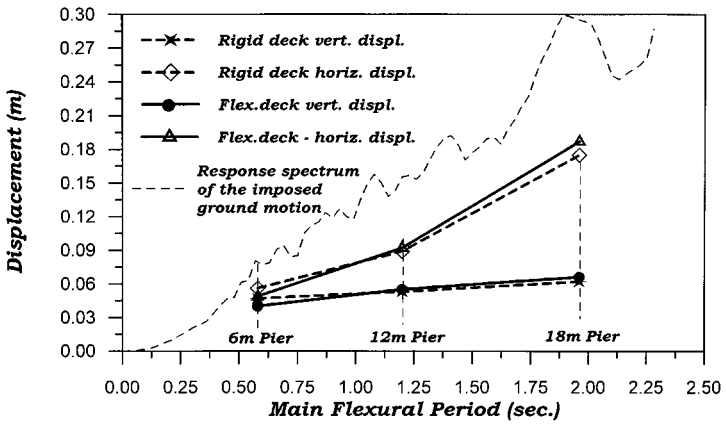

Figure 10

pier flexural response, which is driven by the horizontal mass inertia and does not significantly vary with deck flexibility. The same result is found for the three structures, indicating that deck flexibility has little influence on displacements in a wide range of pier flexural periods.

In the following, the analysis of the frequency content of vertical motion will be carried out for the rigid deck model only, since minor differences are found for the flexible deck case. The plots of Figure 11 show the acceleration response spectra (with 5 per cent damping) of the horizontal and vertical deck motion recorded at each bearing location and at pier top. The ground motion spectrum is plotted for comparison. These spectra provide an idea of the frequency content and magnitude of the structural response. Their values for $T = 0$ correspond to the maximum accelerations plotted in Figures 8 and 9, which are the ones to be used to evaluate the maximum vertical and horizontal force transmitted between deck and piers. In Figure 11, the peak below 0·2 sec at the outer bearing location is clearly due to the selective amplification of the first vertical vibration mode of the pier (see mode 3 in Figure 4(a)). It can be seen that the response spectra of vertical accelerations tend to be more concentrated in a narrow band of frequencies as the pier flexural period increases, while those of horizontal accelerations tend instead to have a constant level of response (i.e. frequency independent) around 0·75 g.

It can be noted from the results discussed above that on external bearings vertical acceleration response is equal or greater (up to a factor of 2 for the 6 m pier) than the horizontal one. With the ratio between vertical and horizontal force on bearings (R_v/H) falling to such low values, unseating phenomena are likely to occur. The most significant examples of these low values occurred during the analysis are reported in Table IV for both internal and external bearing in the 6 m pier. The situation at maximum response ($t = 24{\cdot}54$ sec.) is also reported. Note that the vertical reaction under self-weight alone is equal to 1500 kN.

Response at 8·22 sec shows a case, opposite to the ones discussed above, in which the maximum vertical reaction of the bearings is nearly twice the static one. The full time history of the vertical reaction has been plotted as a function of the corresponding shear force in Figure 12. During the analysis the external bearing experiences a minimum ratio between vertical reaction R_v and shear force H equal to 0·65, while the internal bearing has a minimum value of 2·26.

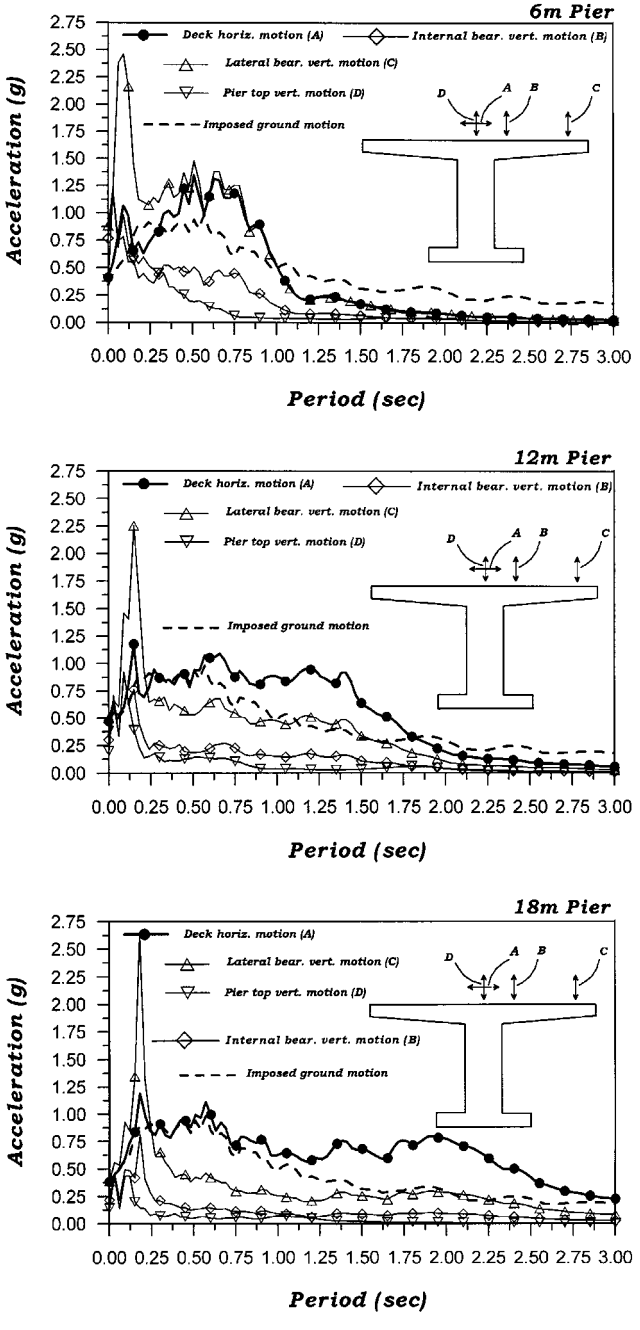

Figure 11

Table IV. Forces on bearings during earthquake response

	External bearing		Internal bearing	
Time (sec)	Shear (kN)	Vert. react. (kN)	Shear (kN)	Vert. react. (kN)
5·23	−469	305	−469	1119
8·22	43	2639	43	1932
8·26	−572	556	−572	1500
24·54	291	1172	291	1388

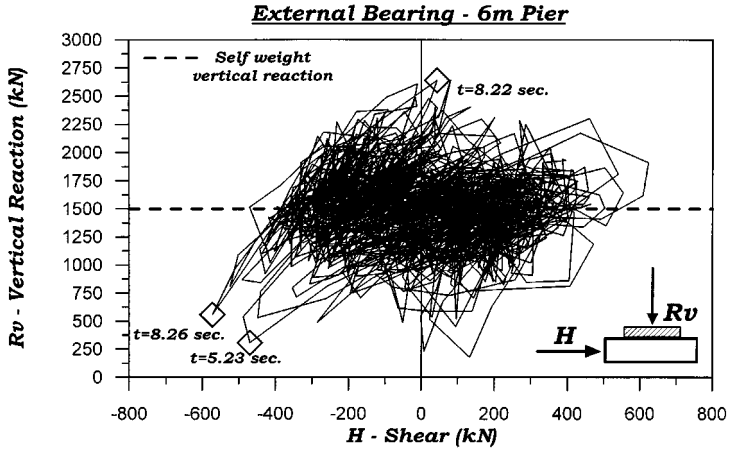

Figure 12

This result confirms that bending-induced axial vibrations can produce severe effects when amplified by the presence of wide cap beams. Moreover, when the pier has a low aspect ratio, the level of axial accelerations induced by flexural cracks is particularly high.

If the time-history analyses of the three structures are repeated using the longitudinal reinforcing ratios found dimensioning according to EC8 (see Table II), lower accelerations are found. Displacement ductilities at maximum response are 2·5, 3·5 and 4·0 for the 6, 12 and 18 m pier, respectively, showing a remarkable accuracy of the EC8 methodology. Vertical accelerations at pier top are 20–25 per cent lower with respect to the piers previously analysed, showing that no direct proportionality can be established between axial impulse and pier ductility. This is confirmed by the fact that a 50 per cent reduction in ductility for the EC8-6 m pier (with respect to the pier of previous analyses) is associated to a 20 per cent reduction of the vertical accelerations while in the EC8-18 m the same reduction in vertical acceleration is associated with a doubling of displacement ductility. It is thus confirmed that the pier aspect ratio and the maximum horizontal acceleration response, rather than the global ductility level, have influence on the axial vibrations.

The effect of the vertical ground motion component can now be introduced to attempt a quantification of the relative importance of the two different sources of axial vibrations.

The analyses carried out above are repeated again for the first set of structures (i.e. allowable stress designed) with inclusion of a vertical motion with peak ground acceleration equal to 2/3 of

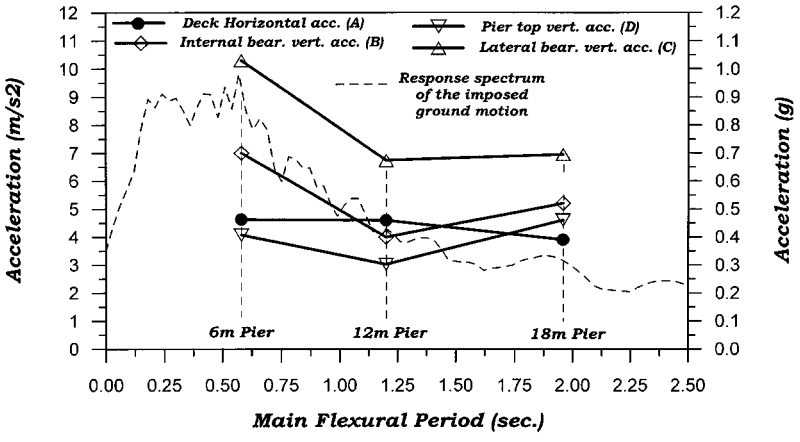

Figure 13. Rigid deck model. Horizontal and vertical seismic input

horizontal peak acceleration. This ground motion component is still compatible with the EC8 response spectrum and has the same duration and starting time step of that of horizontal motion. In these analyses the two sources of axial vibrations are therefore taken into account and their effects appear combined. Maximum acceleration results are reported in Figure 13. The values are in all cases larger than the corresponding ones in Figure 8, where the ground vertical acceleration is absent, but it is perhaps surprising to note that the order of magnitude has not changed. In other words, from the 'spot' cases examined it would seem that the predominant contribution to the vertical response accelerations comes from the rocking mechanism, not from the vertical acceleration input. This is probably a hasty conclusion, not supported by adequate evidence and generality of the cases under consideration, but it is at least an indication that if vertical accelerations are of some consequence for the resistance of bridge piers and deck supports, the rocking mechanism effect should not be neglected.

SIMPLE MECHANICAL MODEL FOR AXIAL VIBRATIONS

An attempt to establish a closed-form approximate relationship between these axial vibrations and the pier flexural response will be presented herein. The main assumption is that cracked sections can be treated as rigid bodies during their motion induced by flexural response. In this idealization the sections rotate about a point that coincides with the position of the neutral axis. The impact of the sections during bending reversal will be assumed elastic with initial conditions (i.e. values of velocity and acceleration) found from the rigid-body motion assumption.

Assuming that plane sections remain plane, the following relation holds between the curvature χ and axial elongation ε_p for a RC section:

$$\varepsilon_p = |\chi| \, (k - \tfrac{1}{2}) \, d \tag{1}$$

where k is a scalar parameter ($0 \leqslant k \leqslant 1$) defining the neutral axis depth $(1 - k)d$.

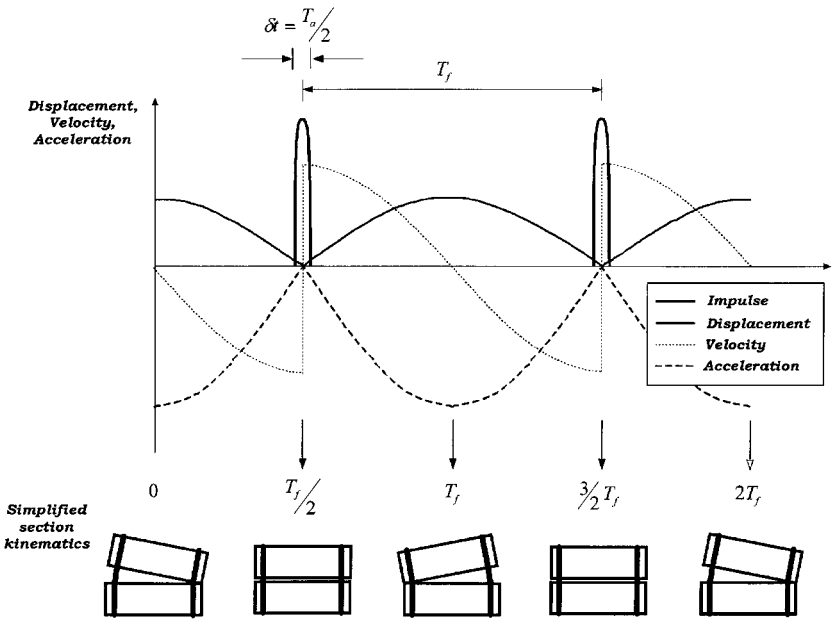

Figure 14

Let us now assume the flexural response of a generic section be described by a simple sinusoidal function as follows:

$$\chi(t) = \chi^{\max} \sin\left(\frac{2\pi t}{T_{\mathrm{f}}}\right) \tag{2}$$

with T_{f} being the predominant flexural period of the pier. The section axial deformation, according to equation (1), can therefore be written as

$$\varepsilon_{\mathrm{p}}(t) = \chi^{\max} \left|\sin\left(\frac{2\pi t}{T_{\mathrm{f}}}\right)\right| (k - \tfrac{1}{2})\, d \tag{3}$$

where the absolute value of the sinusoidal function is taken since the axial elongation is always positive. In order to obtain simple expressions for the velocity and the acceleration of the axial strain (3) we assume that the position of neutral axis is fixed (i.e. k is constant), even though with increasing curvature the neutral axis tends to shift outwards (i.e. k increases). Axial displacement, axial velocity and axial acceleration as a function of time have been qualitatively plotted in Figure 14.

The velocity is discontinuous for $t = nT_{\mathrm{f}}/2$ (with $n = 1,2 \ldots$). In these characteristic points, the section is subjected to a vertical impulse which reverses the displacement direction, changing sign to the axial velocity. These points correspond to the crack closure and the sudden shift of the neutral axis from one side of the section to the other (as depicted in Figure 14 in the section kinematics). These impulses are the main cause of the vertical oscillations observed in the analyses. Outside these points, the section is still subjected to a vertical acceleration

as the result of the flexural response. This component of the acceleration, smaller than the impulsive one at bending reversal, is found as the second derivative of equation (3). Its maximum value is

$$[a^{\max}]_{(t \neq n(T_f/2))} = \left[\left(\frac{d^2\varepsilon_p}{dt^2}\right)^{\max}\right]_{(t \neq n(T_f/2))} = \chi^{\max}\frac{4\pi^2}{T_f^2}(k-\tfrac{1}{2})\,d \tag{4}$$

In the following, it will be shown that this component of the vertical acceleration is negligible when compared to that due to the impulse at bending reversal (see equation (7)).

In order to obtain an estimate for the magnitude of this impulse, the assumption of rigid-body motion must be relaxed and the impact at crack closure treated as an elastic rebound. We assume therefore that this elastic impact takes place in a finite time interval Δt. With these hypotheses, the impulse amplitude can be computed as follows:

$$m\Delta v = \int_{\Delta t} f\,dt = \int_{\Delta t} m\,a\,dt \tag{5}$$

where m is the mass and f the inertia force. The velocity variation Δv that takes place during the time interval Δt can be set according to Figure 14 by computing the right and left limit of the first derivative of equation (3) for $t \to nT_f/2$. The time interval Δt is tentatively set equal to one-half the fundamental axial period of the pier-deck system ($\Delta t = T_a/2$), so that Δt corresponds to the compressive semi-cycle of the pier elastic rebound. Therefore, the velocity variation within the specified time interval is

$$\Delta v = 2\left[\frac{d\varepsilon_p}{dt}\right]_{(t \to n(T_f/2))} = 2\chi^{\max}\frac{2\pi}{T_f}(k-\tfrac{1}{2})\,d \tag{6}$$

If we assume that the impulse has a sinusoidal shape, we obtain from equation (5)

$$[a^{\max}]_{(t=n(T_f/2))} = \frac{\pi}{2}\frac{\Delta v}{\Delta t} = \frac{\pi}{2}\frac{2}{T_a}\chi^{\max}\frac{4\pi}{T_f}(k-\tfrac{1}{2})\,d \tag{7}$$

where the $\pi/2$ factor is found by integrating the sinusoidal impulse over the time interval Δt in equation (5).

A simple relation between the pier maximum horizontal acceleration response and the curvature maximum acceleration can be easily obtained by assuming the flexural deformations taking place in a localized plastic hinge at the column base. In this case we obtain that the maximum acceleration at pier top is

$$a_h = \beta(T_f) = l_{cp}H\left(\frac{d^2\chi}{dt^2}\right)^{\max} = l_{cp}H\chi^{\max}\frac{4\pi^2}{T_f^2} \tag{8}$$

where l_{cp} is the plastic hinge length, H the pier height and $\beta(T_f)$ is the ordinate of the acceleration response spectrum for the pier predominant flexural period. The simplification associated with this kinematic mechanism is valid for single-column bents in general, also for members that tend to oscillate in double bending, because maximum curvature at column base is, in most cases, one order of magnitude greater than that at column top, where yielding of steel seldom occurs.

Similarly, if the largest axial deformations take place within the plastic hinge region, as it is for the plastic rotations, the maximum value of the impulsive ($a_{v,i}$) component of the pier vertical

Table V. Numerical analysis versus equation (10) prediction

Pier height (m)	β_h (m/sec^2)	β_v (m/sec^2)	T_a (sec)	T_f	$(k-1/2)$	$a_{v,i}$ (m/sec^2)	$\beta_v/a_{v,i}$
6	4·12	3·96	0·10	0·69	0·27	3·19	1·24
12	4·72	2·00	0·13	1·21	0·22	2·0	1·00
18	3·83	1·43	0·15	1·92	0·18	1·22	1·17

acceleration can be written as

$$a_{v,i} = l_{cp}\left[\left(\frac{d^2\varepsilon_p}{dt^2}\right)^{max}\right]_{(t=n\,(T_f/2))} = \left(\frac{T_f}{T_a}\right)\beta(T_f)(k-\tfrac{1}{2})\frac{d}{H} \tag{9}$$

The following remarks need to be made:

(1) Equation (9) has been derived by using the velocity reversal found with a rigid section kinematics hypothesis and therefore it should provide an upper bound estimate of the axial impulses
(2) equation (9) should not be taken as an estimate of the structural response in the vertical direction but rather as an estimate of the axial input associated to the flexural response.

However, large amplifications of this vertical input are unlikely since these vertical impulses have the same frequency of the pier flexural response, which is generally smaller than both pier and superstructure vertical frequencies.

The numerical analyses presented above seem to show that, in spite of the crude approximation used in deriving equation (9), it still encompasses the governing variables of the problem. A comparison between the values found with equation (9) and the results of the non-linear analyses for the rigid deck model are presented in the following Table V. Horizontal and vertical accelerations found from time-history analyses are indicated with β_h and β_v, respectively. The flexural period of the piers T_f has been calculated by using the secant flexural stiffness at maximum response (average stiffness). The axial period T_a instead has been computed using the cracked elastic stiffness and the neutral axis depth at maximum response. In this case study, both secant stiffness and neutral axis depth, were available from the results of the non-linear analyses; for design purpose instead, they should be calculated by using the assumed structural ductility or the maximum expected displacement, if a displacement-based design approach is being used.

The results from Table V seem to indicate the soundness of the assumptions used to derive equation (9) and the capability of it to provide a correct estimate of the magnitude of these axial vibrations. This is demonstrated by the stability of the computed values, which show a constant ratio with the results of the non-linear analyses, although referred to piers of different period and different response in both horizontal and vertical direction.

From the cases presented above it seems that little or no amplification of the axial motion is found between pier base and pier top. However, it is important to note that the axial input found with equation (9) might have been overestimated due to the assumption of section rigid-body motion.

Results obtained with equation (9) are strongly affected by the value assumed for $\beta(T_f)$. In our case this value was given by the results of non linear time history analyses (β_h), whereas in design

it must be found from a design spectrum based on the maximum expected ductility (i.e. behaviour factor). Accuracy on $a_{v,i}$ is therefore strongly influenced by the accuracy of the design methodology in estimating the maximum horizontal response.

CONCLUSIONS

Although experimental results are needed to confirm the predictions of the numerical study presented herein, there is no doubt that a significant contribution to the vertical acceleration in RC piers subjected to seismic excitation is due to the rocking mechanism. This contribution is neglected in ordinary design, based on linear modal analysis and response spectra. The intensity of this vertical acceleration may instead be greater than the structural response to the vertical component of the seismic input motion. In fact, the vertical acceleration associated with the rocking mechanism is generated by the horizontal acceleration response of the pier which is always greater than the horizontal ground motion input.

The effect of this additional motion in the vertical direction can be particularly severe on deck bearings, which may experience the maximum horizontal shear forces associated with very low vertical reactions. This mechanism may provide an additional explanation for the widespread phenomenon of bearing failure and deck unseating observed during past earthquakes.

When proposing a simple predictive equation for the quantification of this phenomenon, to be used together with the commonly accepted procedure of seismic design based on modal analysis and response spectra, one should take into account the following features of this mechanism:

1. Direct proportionality seems to exist between bending-induced vertical oscillations and the horizontal acceleration of the pier, while the same cannot be said for flexural damage (i.e. maximum displacement ductility).
2. The structural response to this axial input may have a larger impact than the response to the vertical component of the seismic ground motion since it has the same frequency as the flexural response.

Based on the preliminary investigations presented herein, it seems that equation (9) provides a reasonable estimate of the vertical accelerations in bridge piers of current use subjected to horizontal seismic input motion only. This equation could be used as a starting point towards the definition of a design formula for the quantification of this additional vertical component to be used in the dimensioning of bridges in seismic areas. The effect of maximum ductility and pier cross-section configuration should be further investigated and possibly included in the equation. Results of the present model would greatly benefit from comparisons with experiments performed on shaking tables.

REFERENCES

1. K. Ono, H. Kasai and M. Sasagawa, 'Up-down vibration effects on bridge piers', *Special Issue of Soils and Foundations*, Japanese Geotechnical Society, Chiyoda-ku, Tokyo, 1996, pp. 211–218.
2. A. J. Papazoglou and A. S. Elnashai, 'Analytical and field evidence of the damaging effect of vertical earthquake ground motion', *Earthquake Engng. Struct. Dyn.* **25**, 1109–1137 (1996).
3. A. S. Elnashai and A. J. Papazoglou, 'Procedure and spectra for analysis of RC structures subjected to strong vertical earthquake loads', *J. Earthquake Engng.* **1**(1), 121–155 (1997).
4. B. Mohammadioun, 'Nonlinear response of soils to horizontal and vertical bedrock earthquake motion', *J. Earthquake Engng.* **1**(1), 93–119 (1997).

5. JSCE (Japan Society of Civil Engineers), 'The great Hanshin earthquake, January 17, 1995', *Preliminary Report*, 1995.
6. C. Papalentiou and J. M. Roesset, 'Effect of vertical accelerations on the seismic response of frames', *Structural Dynamics — Eurodyn '93*, Balkema, Rotterdam (1993).
7. A. S. Elnashai, J. J. Bommer, C. I. Baron, D. Lee and A. I. Salama, 'Selected engineering seismology and structural engineering studies of the Hyogo-ken Nambu (Great Hanshin) earthquake of 17 January 1995', *Research Report ESEE-92/2*, Imperial College (1995).
8. M. Petrangeli and P. E. Pinto, 'Finite element modelling of the Hanshin viaduct failure in Kobe', *Proc. 2nd Japan–Italy Workshop on Seismic Design of Bridges*, Rome, Italy (1997).
9. EUROCODE 8 'Design provisions for earthquake resistance of structures', ENV 1998-2: Bridges, CEN, Brussels (1994).
10. M. J. Kowalsky, M. J. N. Priestley and G. A. Macrae, 'Displacement based design of RC bridge columns in seismic regions', *Earthquake Engng. Struct. Dyn.* **24**, 1623–1643 (1995).
11. M. Petrangeli, 'Modelli Numerici per Strutture Monodimensionali in Cemento Armato', *Dissertation*, University of Rome "La Sapienza", Rome, Italy, 1996 (in Italian).
12. M. Petrangeli, P. E. Pinto and V. Ciampi, 'Fiber beam element for cyclic bending and shear of RC structures. I: Theory and II: Verification', *J. Engng Mechanics*, Vol. **125** (1999).
13. M. Petrangeli and V. Ciampi, 'Equilibrium based numerical solutions for the nonlinear beam problem', *Int. J. Numer. Methods Engng.* **40**(3), 423–438 (1997).
14. J. B. Mander, M. J. N. Priestley and R. Park, 'Theoretical stress–strain model for confined concrete', *J. Struct. Engng. ASCE*, **114**(8), 1804–1826 (1988).
15. M. Menegotto and P. E. Pinto, 'Slender RC compressed members in biaxial bending', *J. Struct. Engng. ASCE*, **103**(3), 587–605 (1977).

